RSC Advances

PAPER

View Article Online
View Journal | View Issue

Cite this: *RSC Adv.*, 2020, **10**, 41921

Construction of fluorescence active MOFs with symmetrical and conformationally rigid *N*-2-aryl-triazole ligands†

Jingyang Li,[a] Ying He,[b] Li Wang,[a] Guanghua Li,[a] Yongcun Zou,[a] Yan Yan,[a] Dandan Li,[a] Xinli Shi,[a] Zhiguang Song*[a] and Xiaodong Shi*[b]

Received 1st November 2020
Accepted 5th November 2020

DOI: 10.1039/d0ra09305j

rsc.li/rsc-advances

1,4-Bis-triazole-substituted arene (NAT) was designed and synthesized for the construction of metal organic frameworks. Unlike the tri-phenyl analogs, which give a twisted conformation between three benzene rings due to the A-1,3 repulsion, the NAT-ligand gave the energetically favored co-planar conformation with the strong fluorescence emission. With this ligand, two new MOFs, NAT-MOF-Cd (2,3,4-c) and NAT-MOF-Cu (4-c), were successfully obtained with the structure confirmed by X-ray. With the six-coordinated Cd(II) cluster, an interesting metal–ligand coordination and H-bonding hybridized porous polymeric structures were observed. In contrast, a typical Cu(II) paddle wheel coordination was obtained with NAT and Cu, giving a new MOF structure with moderate stability in aqueous solution from pH 1–11 for 24 hours, which suggests a promising future for applications in fluorescence sensing and photocatalysis.

With large surface areas, diverse geometries, tunable pore sizes, and accessible functional sites, metal organic frameworks (MOFs) have shown exciting applications in various research areas, including gas molecule storage and separation, chemical catalysis, molecular sensing, luminescence, drug delivery, optical/electronic devices, *etc.*[1] From the design perspective, the geometry of the ligand is crucial for the overall network construction and its function.[2] Over the past decade, our group has been focusing on the investigations of 1,2,3-triazole derivatives for applications in chemical synthesis and material preparation.[3] These efforts have led to the discovery of interesting new functions associated with certain triazole analogs. One particularly interesting building block is the *N*-2-aryl-1,2,3-triazole (NAT) moiety recently reported from our lab.[4] Unlike the ubiquitous N-1 isomers, which were prepared from CuAAC (click chemistry), the NATs have shown excellent co-planar conformation between triazole and arene rings.[5] As a result, NAT gives strong fluorescence while N-1 isomer shows almost no emission.[6] Both the unique structure and interesting photo activity makes NAT interesting molecular building blocks in materials development.[4] Herein, we report two new NAT based MOFs with moderate water (acid/base) stability and fluorescence emissions.

Our interest in NAT-MOF synthesis was initiated by the realization of twisted conformation associated with the polyarene system. It is well-known that spacing linkers are important in MOF design to alter pore size.[7] Considering the required structure rigidity often required for stable MOF structure, polyarenes are one very popular linker motif.[8] However, as shown in Scheme 1A, the typical bi-aryl molecule could not adopt co-planar conformation due to the A-1,3 repulsion between the *ortho*-protons on adjacent benzene rings.[9] As a result, two conformations could be adopted: (A) twisted (all three rings twisted) and (B) orthogonal (rings 1 and 3 are parallel and twisted the same angle with ring 2).[10] Overall, it is impossible to

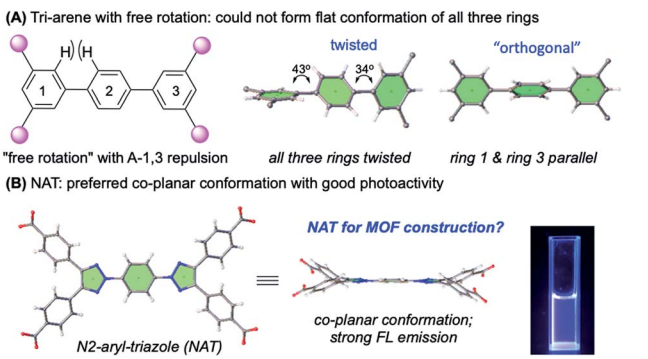

Scheme 1 Tri-aryl linker in MOF construction: twisted conformation.

[a]*State Key Laboratory of Supramolecular Structure and Materials, College of Chemistry, Jilin University, Changchun, Jilin 13002, China. E-mail: szg@jlu.edu.cn*

[b]*Department of Chemistry, University of South Florida, 4202 E. Fowler Avenue, Tampa, Florida 33620, USA. E-mail: xmshi@usf.edu*

† Electronic supplementary information (ESI) available. CCDC 2024239 and 2009548. For ESI and crystallographic data in CIF or other electronic format see DOI: 10.1039/d0ra09305j

have all three aryl rings lining up to form a planar conformation, which could be crucial to open the window for effective π–π stacking. In contrast, with a coplanar conformation, NAT could serve an interesting and ideal new ligand for the extended poly-arene linker MOF construction. Besides the structure novelty, two other important concerns for MOF construction are material stability and practical ligand synthesis for potential applications.[11] With low electron density, 1,2,3-triazole is very stable toward oxidative conditions.[12] Moreover, the *N*-2-substitution successfully avoid potential triazole ring opening through N_2 extrusion.[13] We then put in our efforts to develop a practical synthesis of the triazole-arene ligands. After evaluating various protecting groups and reaction sequences, a general route was developed as shown in Fig. 1.

The synthesis starts from commercial available 4,5-dibromotriazole **1**. Protecting triazole with PMB group followed by the Suzuki coupling gave 4,5-diaryl triazole in excellent overall yields. Deprotection of PMB group gave NH triazole **2**, which was applied to copper mediated Ullman coupling to afford the tetra-esters. Saponification followed by recrystallization gave the tetra-acid NAT ligand. Overall this route could afford the desired NAT ligand in gram scale with five linear steps. The resulting NAT tetra-acid is fluorescence active both in solution and in a solid state as expected. Notably, this route could be easily applied to the coordination with other linkers (besides benzene) for the coordination of new functional groups into the central arene, which is currently under investigation in our lab. With tetra-acid NAT available, we explore the possibility of applying them in MOF construction through coordination with two typical cations, Cd^{2+} from group 12 and Cu^{2+} from group 11. Fortunately, both complexes were successfully obtained under typical MOF preparation conditions (see details in ESI†). The X-ray crystal structures of both MOFs were successfully obtained.

As shown in Fig. 2, NAT-MOF-Cd was prepared through solvothermal condensation with NAT ligand and $Cd(NO_3)_2$ in the mixture of DMF, EtOH, water, and HNO_3 (5 : 1 : 1 : 1) at 85 °C. The needle-like transparent crystal was obtained. X-ray crystal structure reveals the typical 7-coordinated Cd cluster from three carboxylates and one DMF (Fig. 2A). Interestingly, as a tetra-acid ligand in coordination with a six-coordinated Cd cluster, the NAT ligand shows two different coordination patterns. For NAT-1, both carboxylates on each end of the ligand coordinated with Cd^{2+}, forming cycle I (9.5 Å × 13.7 Å) through binding with neighboring NAT-1. On the other hand, only one carboxylate on each side of NAT-2 ligand coordinates with Cd^{2+}

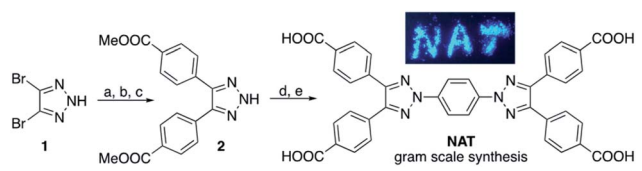

Fig. 1 Synthesis of NAT ligands: (a) PMBBr (1.1 equiv.), K_2CO_3 (4 equiv.), MeCN, 60 °C, 96%; (b) *p*-$B(OH)_2$–C_6H_4–COOMe, 5% $Pd(PPh_3)_4$, K_2CO_3 (4 equiv.), 1,4-dioxane : H_2O(1 : 1), 100 °C, 97%; (c) TFA, 120 °C, 54%; (d) 1,4-phenylenediboronic acid (0.5 equiv.), $Cu(OAC)_2$ (1.5 equiv.), pyridine (2 equiv.), THF, 1 atm O_2, 70 °C, 50%; (e) KOH, MeOH : THF (1 : 1), 100 °C, 90%.

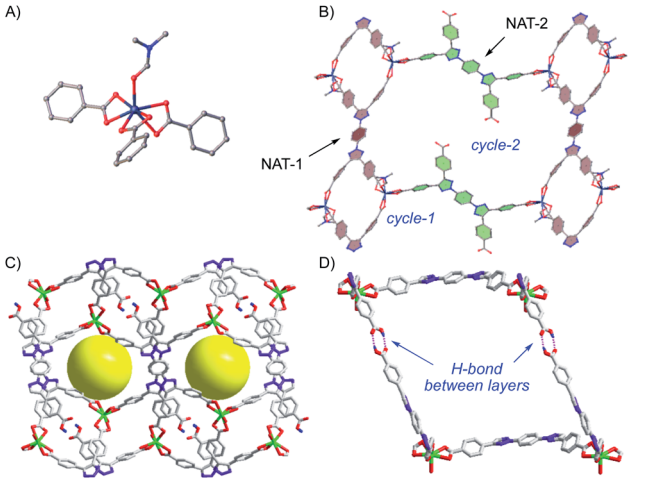

Fig. 2 (A) coordination environments of both ligand and Cd(II) ions; (B) two coordination patterns of NAT-1 and NAT-2; (C) 3D packing view of NAT-MOF-Cd along *b* axes with fitted pores; (D) layer-by-layer H-bonded framework of NAT-MOF-Cd.

(to satisfy the overall six-coordination Cd cluster). The NAT-2 binding with Cd-SBU not only links the cycle 1 but also produces metallocycle 2 with a larger size (23.2 Å × 33 Å). As expected, both NAT-1 and NAT-2 show good co-planar conformation with the dihedral angle <30° in both cases, which highlight the unique structural feature of NAT over poly-arenes. While the cycle-1 and cycle-2 form large network extension, it is overall a 2D layer structure (Fig. 2B). However, with the uncoordinated free COOH in NAT-2, a layer-by-layer hydrogen bonded metal organic framework was achieved. As a result, the overall 3D packing framework is composed of layer-by-layer H-bonding and vertical six-coordinated Cd(II) cluster MOF along the *b* axis as shown in Fig. 2C. The H-bond between COOH of each layer ($d_{OH\cdots O} = 2.623$ nm) is confirmed and perfectly lining up the open cavity, forming cylindrical pores in the vertical direction (Fig. 2D).

The topology of this new NAT-MOF-Cd is calculated to be 2,3,4-c net with stoichiometry (2-c)(3-c)2(4-c) while the point (Schlafli) symbol is $\{4\cdot8^2\}2\{4^2\cdot8^2\cdot10^2\}\{8\}$. The PXRD of the crystal structure was uniform with simulated data (Fig. S3a†). FT-IR of NAT-MOF-Cd (Fig. S5a†) showed the disappearing of 2990 cm^{-1} adsorption associated with carboxylic acid and the appearance of 1390 cm^{-1} and 1590 cm^{-1} signal associated with the symmetric and asymmetric stretching of carboxylates. Thermogravimetric analyses (TGA) revealed the good thermal stability of NAT-MOF-Cd up to 351 °C (no decompositions) and completely collapsed at around 456 °C (Fig. S6a†).

The successful synthesis of NAT-MOF-Cd confirmed our hypothesis that fluorescence active NAT ligand could be used as a novel co-planar linker to coordinate with secondary building units (SBU) for porous MOF construction. The three-dimensional H-bonded MOF structure is interesting molecular architecture. However, it raised the concern whether it will be stable in an aqueous solution where many applications are taking place. Soaking NAT-MOF-Cd in water for only 30 minutes caused a total collapse of MOF structures confirmed by PXRD

(Fig. S4†). To achieve more rigid MOF structures with this NAT, we put our attention to Cu^{2+}. It is well known that Cu(II) cations could coordinate with four carboxylates to form a paddle wheel SBU. The good match of tetra-acid and four-coordinated Cu makes NAT ligand ideal for MOF construction *via* Cu-SBU. After screening various conditions, we were pleased to identify the combination of NAT with $Cu(NO_3)_2 \cdot 3H_2O$ (1 : 2) in a mixture of DMF, EtOH, water, and AcOH (5 : 1 : 1 : 1) as the optimal conditions for MOF synthesis. The FT-IR spectra (Fig. S5b†) of resulting MOF revealed the disappearance of carboxylic acid groups around 2983 cm^{-1} and the symmetric and asymmetric stretching of carboxylate groups at 1394 cm^{-1} and 1581 cm^{-1}. The cubic-shape blue crystal was obtained with the structure confirmed by X-ray.

As revealed by X-ray, the NAT-MOF-Cu is constructed with a typical Cu(II) paddle wheel SBU (Fig. 3A). Each paddle wheel is coordinated with carboxylates from four NAT with two DMF bound on the *c* direction (Fig. 3B). Similar to NAT-MOF-Cd, the ligand in NAT-MOF-Cu shows good co-planar conformation with the dihedral angle <30°. The overall packing structure with pores along the *c* axis of NAT-MOF-Cu is shown in Fig. 3C. Meanwhile, the topology of NAT-MOF-Cu is calculated to be 4-c net with the point (Schlafli) symbol of $\{4^4 \cdot 6^2\}$. The PXRD pattern was consistent with the simulated curve of the crystal structure (Fig. S3b†). Thermalgravimetric analyses confirmed the thermal stability of NAT-MOF-Cu that it could behave intact as crystal scaffold until 354 °C before completely decomposed at around 551 °C (Fig. S6b†).

The porosity of both NAT-MOFs was identified by CO_2 adsorption at 195 K. The framework behaves reversible type-I isotherm adsorption features, in which gas molecules present sharp adsorption at relatively low pressure ($P/P_0 < 0.1$) and reach to a plateau at 131 $cm^3\ g^{-1}$ with NAT-MOF-Cu (Fig. 3D). The Brunauer–Emmett–Teller (BET) and Langmuir surface area were calculated to be 309 $m^2\ g^{-1}$ and 436 $m^2\ g^{-1}$ for NAT-MOF-Cu

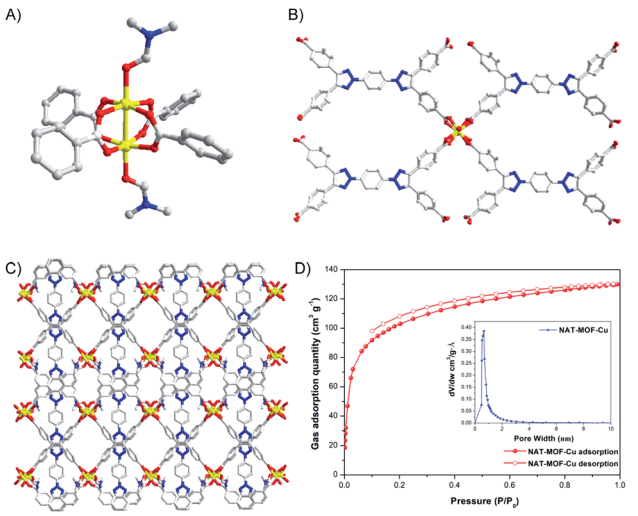

Fig. 3 (A) Paddle wheel SBU of NAT-MOF-Cu; (B) coordination environments of NAT-MOF-Cu; (C) 3D packing view of NAT-MOF-Cu along c axes; (D) CO_2 sorption and pore volumes of NAT-MOF-Cu at 195 K.

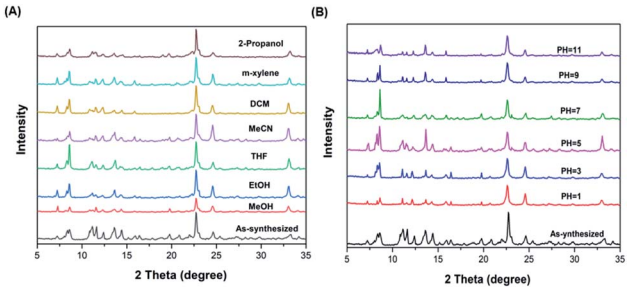

Fig. 4 Solvent stability tests of NAT-MOF-Cu in (A) organic solution and (B) aqueous solution.

because of large pore volumes from Horvath-Kawazoe calculation mode and regular stacking. Gas adsorptions of CO_2 and N_2 for NAT-MOF-Cu at 273 K were also obtained (Fig. S7b†). The maximum adsorption of CO_2 was 43 $cm^3\ g^{-1}$ and the value of CO_2/N_2 selectivity (Fig. S7d†) was obtained as 44.2 by ideal solution adsorbed theory (IAST) with a good correlation factor ($R^2 > 0.999$). Gas adsorption including BET surface area (37 $m^2\ g^{-1}$) and CO_2/N_2 selectivity (8.5) at 273 K of NAT-MOF-Cd was also measured. Detailed figures are provided in ESI (Fig. S7 and S8†).

The stability of both NAT-MOFs was evaluated. As demonstrated previously, with the layer-by-layer H-bond, NAT-MOF-Cd is not stable in protic solvents. In contrast, the NAT-MOF-Cu showed excellent stability. First, immersing NAT-MOF-Cu in various organic solvents, including MeOH, EtOH, THF, MeCN, DCM, *m*-xylene, and 2-propanol, at room temperature for 24 h showed no crystal decomposition based on crystal PXRD (Fig. 4A). Furthermore, stability in aqueous solution under different pH was also evaluated by soaking the MOF in the aqueous solutions. NAT-MOF-Cu showed almost no decomposition in aqueous media with pH from 1 to 11 (Fig. 4B). Further increasing to pH = 13 or reducing to pH = 0 did give complex decomposition over time. However, the ability to survive aqueous solution over a large pH range showed the good stability of this new NAT-MOF-Cu porous materials.

In general, the formation of carboxylate MOF complexes could enhance ligand fluorescence intensity due to the locked conformation that prevents undesired excitation state relaxation. NAT-MOF-Cd showed enhanced fluorescence (Φ = 26%) compared with NAT ligand (Φ = 6.7%) in solid state (Fig. 5). Interestingly, NAT-MOF-Cu gave significant fluorescence

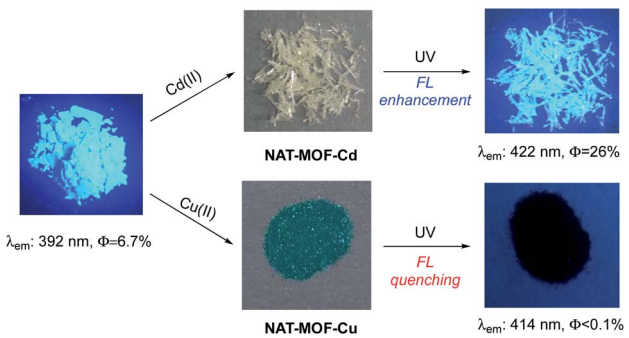

Fig. 5 Solid state fluorescence emission of NAT and NAT-MOFs.

quenching with the resulting MOF showed almost no emission (Φ < 0.1%). This result suggested plausible electron or charge transfers in the excitation state with this new MOF material. The exact mechanism is currently under investigation along with the potential application of this new photoactive MOF as sensor or photocatalysts. The results will be reported in due course. Nevertheless, the intrinsic photoactivity along with the co-planar conformation makes NAT a promising new ligand system for future porous material construction.

In summary, we designed and synthesized 1,4-bis-triazole-substituted arene (NAT) as a new ligand for the construction of metal organic frameworks. Compared with poly-arenes system, NAT adopts co-planar conformation with the dihedral angle <30°. NAT-MOF-Cd (2,3,4-c) was formed by six-coordinated Cd(II) clusters with interesting H-bonded MOF framework while NAT-MOF-Cu (4-c) was obtained with Cu(II) paddle wheel SBU. NAT-MOF-Cu showed reasonable stability in wide pH range (1–11) and organic solvent for over 24 h. Photoluminescence properties were observed upon the formation of NAT-MOF, suggesting potential applications of this photoactive porous material through the new ligand design.

Conflicts of interest

There are no conflicts to declare.

Acknowledgements

We are grateful to Jilin Province (20170307024YY and 20190201080JC) for financial support.

Notes and references

1 (*a*) O. M. Yaghi, M. O'Keeffe, N. W. Ockwig, H. K. Chae, M. Eddaoudi and J. Kim, *Nature*, 2003, **423**, 705–714; (*b*) M. E. Davis, *Nature*, 2002, **417**, 813–821; (*c*) H. Li, M. Eddaoudi, M. O'Keeffe and O. M. Yaghi, *Nature*, 1999, **402**, 276–279; (*d*) T. D. Bennett, Y. Yue, P. Li, A. Qiao, H. Tao, N. G. Greaves, T. Richards, G. I. Lampronti, S. A. T. Redfern, F. Blanc, O. K. Farha, J. T. Hupp, A. K. Cheetham and D. A. Keen, *J. Am. Chem. Soc.*, 2016, **138**, 3484–3492; (*e*) Y. Zhao, S. Qi, Z. Niu, Y. Peng, C. Shan, G. Verma, L. Wojtas, Z. Zhang, B. Zhao, Y. Feng, Y. Chen and S. Ma, *J. Am. Chem. Soc.*, 2019, **141**, 14443–14450; (*f*) A. M. Plonka, Q. Wang, W. O. Gor-don, A. Balboa, D. Troya, W. W. Guo, C. H. Sharp, S. D. Sena-nayake, J. R. Morris, C. L. Hill and A. I. Frenkel, *J. Am. Chem. Soc.*, 2017, **139**, 599–602.

2 (*a*) D. Zhao, D. J. Timmons, D. Yuan and H. Zhou, *Acc. Chem. Res.*, 2011, **44**, 123–133; (*b*) M. J. Cliffe, E. Castillo-Martínez, Y. Wu, J. Lee, A. C. Forse, F. C. N. Firth, P. Z. Moghadam, D. Fairen-Jimenez, M. W. Gaultois, J. A. Hill, O. V. Magdysyuk, B. Slater, A. L. Goodwin and C. P. Grey, *J. Am. Chem. Soc.*, 2017, **139**, 5397–5404; (*c*) J. Shen, P. Liao, D. Zhou, C. He, J. Wu, W. Zhang, J. Zhang and X. Chen, *J. Am. Chem. Soc.*, 2017, **139**, 1778–1781; (*d*) Z. Yin, Y. Zhou, M. Zeng and M. Kurmoo, *Dalton Trans.*, 2015, **44**, 5258–5275; (*e*) G. K. Kole and J. J. Vittal, *Chem. Soc. Rev.*, 2013, **42**, 1755–1775.

3 (*a*) R. Cai, W. Yan, M. G. Bologna, K. de Silva, Z. Ma, H. O. Finklea, J. L. Petersen, M. Li and X. Shi, *Org. Chem. Front.*, 2015, **2**, 141–144; (*b*) R. Cai, D. Wang, Y. Chen, W. Yan, N. R. Geise, S. Sharma, H. Li, J. L. Petersen, M. Li and X. Shi, *Chem. Commun.*, 2014, **50**, 7303–7305; (*c*) W. Gao, R. Cai, L. Meng, L. Wojtas, W. Zhou, T. Yidirim, X. Shi and S. Ma, *Chem. Commun.*, 2013, **49**, 10516–10518; (*d*) W. Gao, W. Yan, R. Cai, K. Williams, A. Salas, L. Wojtas, X. Shi and S. Ma, *Chem. Commun.*, 2012, **48**, 8898–8900; (*e*) R. Cai, X. Ye, Q. Sun, Q. He, Y. He, S. Ma and S. Shi, *ACS Catal.*, 2017, **7**, 1087–1092; (*f*) X. Ye, C. Xu, L. Wojtas, N. Akhmedov, H. Chen and X. Shi, *Org. Lett.*, 2016, **18**, 2970–2973.

4 (*a*) J. Li, Y. He, L. Wang, Q. Pan, Z. Song and X. Shi, *Dalton Trans.*, 2020, **49**, 5429–5433; (*b*) Y. Zhang, X. Ye, J. L. Petersen, M. Li and X. Shi, *J. Org. Chem.*, 2015, **80**, 3664–3669.

5 (*a*) Q. Lai, Q. Liu, Y. He, K. Zhao, C. Wei, L. Wojtas, X. Shi and Z. Song, *Org. Biomol. Chem.*, 2018, **16**, 7801–7805; (*b*) W. Yan, Q. Wang, Q. Lin, M. Li, J. L. Petersen and X. Shi, *Chem.–Eur. J.*, 2011, **17**, 5011–5018.

6 (*a*) Y. Liu, W. Yan, Y. Chen, J. L. Petersen and X. Shi, *Org. Lett.*, 2008, **10**, 5389–5392; (*b*) Q. Lai, Q. Liu, K. Zhao, C. Shan, L. Wojtas, Q. Zheng, X. Shi and Z. Song, *Chem. Commun.*, 2019, **55**, 4603–4606.

7 (*a*) L. Ma, J. M. Falkowski, C. Abney and W. Lin, *Nat. Chem.*, 2010, **2**, 838–846; (*b*) Z. Chen, K. Adil, L. J. Weseliński, Y. Belmabkhout and M. Eddaoudi, *J. Mater. Chem. A*, 2015, **3**, 6276–6281; (*c*) L. K. Cadman, J. K. Bristow, N. E. Stubbs, D. Tiana, M. F. Mahon, A. Walsh and A. D. Burrows, *Dalton Trans.*, 2016, **45**, 4316–4326; (*d*) J. Jiao, H. Liu, D. Bai and Y. He, *Inorg. Chem.*, 2016, **55**, 3974–3979; (*e*) A. S. Palakkal and R. S. Pillai, *J. Phys. Chem. C*, 2020, **124**, 16975–16989; (*f*) H. Wang, J. Peng and J. Li, *Chem. Rec.*, 2016, **16**, 1298–1310.

8 (*a*) A. Schoedel, M. Li, D. Li, M. O'Keeffe and O. M. Yaghi, *Chem. Rev.*, 2016, **116**, 12466–12535; (*b*) T. Liu, D. Feng, Y. Chen, L. Zou, M. Bosch, S. Yuan, Z. Wei, S. Fordham, K. Wang and H. Zhou, *J. Am. Chem. Soc.*, 2015, **137**, 413–419; (*c*) Z. Amghouz, S. García-Granda and J. R. García, *Inorg. Chem.*, 2012, **51**, 1703–1716; (*d*) Y. Yan, S. Yang, A. J. Blake and M. SchrÖder, *Acc. Chem. Res.*, 2014, **47**, 296–307.

9 (*a*) R. J. Marshall, C. T. Lennon, A. Tao, H. M. Senn, C. Wilson, D. Fairen-Jimenez and R. S. Forgan, *J. Mater. Chem. A*, 2018, **6**, 1181–1187; (*b*) F. Johnson, *Chem. Rev.*, 1968, **68**, 375–413; (*c*) B. Wang, X. Lv, D. Feng, L. Xie, J. Zhang, M. Li, Y. Xie, J. Li and H. Zhou, *J. Am. Chem. Soc.*, 2016, **138**, 6204–6216.

10 (*a*) L. Lu, J. Wu, J. Wang, J. Liu, B. Li, A. Singh, A. Kumar and S. R. Batten, *CrystEngComm*, 2017, **19**, 7057–7067; (*b*) X. Lin, J. Jia, X. Zhao, K. M. Thomas, A. J. Blake, G. S. Walker, N. R. Champness, P. Hubberstey and M. SchrÖder, *Angew. Chem., Int. Ed.*, 2006, **45**, 7358–7364; (*c*) X. Lin, I. Telepeni, A. J. Blake, A. Dailly, C. M. Brown, J. M. Simmons,

M. Zoppi, G. S. Walker, K. M. Thomas, T. J. Mays, P. Hubberstey, N. R. Champness and M. SchrÖder, *J. Am. Chem. Soc.*, 2009, **131**, 2159–2171; (*d*) J. Yang, L. Zhang, X. Wang, R. Wang, F. Dai and D. Sun, *RSC Adv.*, 2015, **5**, 62982–62988.

11 (*a*) A. V. Desai, B. Manna, A. Karmakar, A. Sahu and S. K. Ghosh, *Angew. Chem., Int. Ed.*, 2016, **55**, 7811–7815; (*b*) M. Ding, X. Cai and H. Jiang, *Chem. Sci.*, 2019, **10**, 10209–10230; (*c*) X. Xie, Y. Yang, B. Dou, Z. Li and G. Li, *Coord. Chem. Rev.*, 2020, **403**, 213100; (*d*) L. Wang, H. Xu, J. Gao, J. Yao and Q. Zhang, *Coord. Chem. Rev.*, 2019, **398**, 213016; (*e*) M. Ding, R. W. Flaig, H. Jiang and O. M. Yaghi, *Chem. Soc. Rev.*, 2019, **48**, 2783–2828.

12 (*a*) B. Sen, S. K. Sheet, S. K. Patra, D. Koner, N. Saha and S. Khatua, *Inorg. Chem.*, 2019, **58**, 9982–9991; (*b*) G. Ding, A. Mahmood, A. Tang, F. Chen and E. Zhou, *Chem. Phys.*, 2018, **500**, 67–73; (*c*) Y. Wang, C. Wei and Z. Song, *Chem. Res. Chin. Univ.*, 2018, **34**, 923–928; (*d*) T. Duan, K. Fan, Y. Fu, C. Zhong, X. Chen, T. Peng and J. Qin, *Dyes Pigm.*, 2012, **94**, 28–33.

13 (*a*) Y. Yang, J. Yu, X. Ouyang and J. Li, *Org. Lett.*, 2017, **19**, 3982–3985; (*b*) W. Li and J. Zhang, *Chem.–Eur. J.*, 2020, **26**, 11931–11945.